

Furthermore, the interpretation of the spectra in Figure 4 favors the following identification of these isomers as ionized and neutral phenylsilylene, C_6H_5SiH .

In the charge-reversal spectrum, Figure 4a, the peak at m/z 105 corresponds to H^+ loss which is expected from the scission of the Si-H bond (which is weaker than the C-H bond). A m/z 77 peak, $C_6H_5^+$, would arise from the scission of the C-Si bond in $C_6H_5SiH^{++}$ with charge transfer from the SiH unit to the phenyl ring (there is no simple cleavage which produces SiC_4H^+ which also has m/z 77). The large peak at m/z 53 can be accounted for by the formation of $SiC_2H^+ + C_4H_5^+$ or their charge-inversed counterparts. Again, such a dissociation follows from the $C_6H_5SiH^{++}$ isomer II if the α C-C bond is broken which causes the localization of the double bonds so that the fragmentation of a C_2 unit connected to Si is favored. The strong H^+ loss and SiH^+ loss appear to be and should be specific to the C-H insertion isomer, C_6H_5SiH . SiC_2H^+ , on the other hand, is also an expected fragment of the ionic ring-insertion isomer because of the conjugated nature of the ring, so that the presence of some of this isomer in the CR spectrum cannot be ruled out. Similar interpretations apply to the NRMS spectrum given in Figure 4b. Similar bond rupture is expected in the neutralization of the ion so that reionization establishes the same spectrum as that obtained by charge reversal.

A small but clearly recognizable recovery signal is again observed. Nevertheless, its presence attests to the stability of neutral C_6H_5SiH for which some spectroscopic evidence also has been reported.⁷ The theoretical investigation indicates a structure for the neutral very similar to that of the ion and an adiabatic ionization energy of 6.8 eV at 0 K.¹²

Conclusions

(1) Theory predicts that the lowest energy isomer thermodynamically accessible to the interaction of Si^{++} and benzene is the π -complex so that a π -structure is expected for the adduct formed in the thermal reaction of Si^{++} with benzene under both the CI conditions employed in this study and the SIFT experiments reported by Bohme et al.²

(2) Neutralization-reionization experiments provide evidence for the presence of at least two distinct isomers of the adduct of Si^{++} and benzene, the π -complex, and the C-H insertion isomer, and their neutral counterparts $Si-C_6H_6$ and C_6H_5SiH . Theory has provided structures, charge distributions, and energies for these two ionic and two neutral isomers, as well as for the neutral and ionized ring-insertion isomers, and predicts the stability order $Si^{++}-C_6H_6 > C_6H_5SiH^{++} > c-SiC_6H_6^{++}$ for the ions and $C_6H_5SiH > c-SiC_6H_6 > Si-C_6H_6$ for the neutrals.

Acknowledgment. Financial support of our work by the Deutsche Forschungsgemeinschaft and the Fonds der Chemischen Industrie is appreciated. R.S. acknowledges the receipt of a visiting fellowship from the Deutscher Akademischer Austauschdienst (DAAD) and the encouragement of Dr. A. V. Rama Rao, Director, ICT, Hyderabad, India. D.K.B. is grateful to the Alexander-von-Humboldt Foundation for a Humboldt Senior Scientist Award and to Professor H. Schwarz for his hospitality.

Registry No. $C_6H_5SiH^+$, 139313-00-1; $Si^{++}-C_6H_6$, 139313-01-2; $C_6H_5SiH^{++}$, 139313-02-3; $c-SiC_6H_6^{++}$, 139313-03-4; C_6H_5SiH , 102389-83-3; $c-SiC_6H_6$, 139313-04-5; $Si-C_6H_6$, 139313-05-6; tetramethylsilane, 75-76-3; benzene, 71-43-2; phenylsilane, 694-53-1.

Nitrogen versus Fluorine Protonation of NF_3 in the Gas Phase. A Combined Mass Spectrometric and GAUSSIAN-1 ab Initio MO Study Reveals the Existence of Two Distinct Isomers F_3NH^+ and F_2N-FH^+

Felice Grandinetti,[†] Jan Hrušák,[‡] Detlef Schröder, Sigurd Karrass, and Helmut Schwarz*

Contribution from the Institut für Organische Chemie der Technischen Universität Berlin, Strasse des 17. Juni 135, W-1000 Berlin 12, Germany. Received October 4, 1991

Abstract: The potential energy surface of $[N,F_3,H]^+$ ions, generated by the gas-phase protonation of NF_3 using CH_5^+ and H_3^+ , is probed by means of high-level GAUSSIAN-1 ab initio MO studies and mass-spectrometric techniques. The global minimum corresponds to the fluorine-protonated isomer F_2N-FH^+ (1). This ion/dipole complex is found to be 6.4 kcal mol⁻¹ more stable than its nitrogen-protonated form F_3NH^+ (2). The barrier for the reaction 1 \rightarrow 2 is significant (52.6 kcal mol⁻¹), thus preventing facile isomerization. Further, while the isomer F_2N-FH^+ has a low energy dissociation channel to produce NF_2^+ and HF, with a heat of reaction of <14.6 kcal mol⁻¹, the less stable isomer F_3NH^+ (2) is trapped in a deep potential well, which prevents both rapid isomerization and dissociation. The potential energy surface explains the distinctly different kinetic energy releases (KER's) associated with the reaction: $[N,F_3,H]^+ \rightarrow NF_2^+ + HF$. The loss of HF from the ion/dipole complex F_2N-FH^+ gives rise to a small KER ($T_{<0.5>} = 21$ meV), while the same reaction of F_3NH^+ (2) is associated with a dish-top peak and a large KER ($T_{<0.5>} = 740$ meV).

Introduction

The question of the protonation site of nitrogen fluoride, NF_3 , has been recently addressed by Fisher and McMahon^{1a} in the context of a study of the intriguing gas-phase ion chemistry of

NF_3/CH_4 mixtures. In addition to the remarkable insertion of NF_2^+ into CH bonds of CH_4 to eventually generate $HCNH^+$, protonated NF_3 was formed, and the reactivity pattern in ion/molecule reactions was found to be consistent with the existence of fluorine-protonated isomer F_2N-FH^+ (1) rather than a nitrogen-protonated ion F_3NH^+ (2). Additional structural evidence

[†] Permanent address: Istituto di Chimica Nucleare del CNR, Area della Ricerca di Roma, C.P. 10 00016 Monterotondo Stazione (Rome), Italy.

[‡] Permanent address: Institute of Macromolecular Chemistry, Czechoslovak Academy of Sciences, Heyrovsky Sq. 2, CS-16202 Prague (Czechoslovakia).

(1) (a) Fisher, J. J.; McMahon, T. B. *J. Am. Chem. Soc.* **1988**, *110*, 7599. (b) For a theoretical study of F_3NH^+ (C_{3v}), also see: Reed, A. E.; Schleyer, P. v. R. *J. Am. Chem. Soc.* **1987**, *109*, 7362.

for $\text{F}_2\text{N}-\text{FH}^+$ (m/z 72) was obtained from a collisional activation (CA) experiment of m/z 72 derived from proton-transfer chemical ionization of NF_3 using CH_5^+ . These results were supported by ab initio MO calculations, which showed the fluorine-protonated isomer **1** to be more stable than the nitrogen-protonated form **2** by 2.2 kcal mol⁻¹ at the 6-31G** + ZPE (6-31G**) SCF level of theory.^{1a}

In view of the difference of the proton affinity (PA) of methane (131.6 kcal mol⁻¹)² and NF_3 , 136.9 kcal mol⁻¹, as obtained by pulsed electron-beam high pressure mass spectrometry,³ and the computed small energy difference between **1** and **2**, it is conceivable that two isomers of protonated NF_3 rather than one species are obtained by protonation with CH_5^+ .

The fact, however, that in the above referenced work^{1a,3} evidence for one isomer only was reported has two implications: (i) both **1** and **2** are formed upon protonation of NF_3 with CH_5^+ ; however, the transition structure **3** for the interconversion **1** → **2** is not high enough to prevent facile isomerization prior to the structural characterization of $[\text{N},\text{F}_3,\text{H}]^+$. In previous work¹ no attempts were made to precisely locate and characterize the transition structure **3**. (ii) Alternatively, one may argue that **1** and **2** are formed in the protonation of NF_3 and both isomers are separated by a significant barrier; the experimental methods used,^{1,3} however, may not be adequate to permit an unequivocal distinction and characterization of the individual isomers **1** and **2**.

In order to resolve this dilemma we performed a more detailed investigation aimed at (i) theoretically describing in greater detail the potential energy surface of $[\text{N},\text{F}_3,\text{H}]^+$ ions (in particular **1**, **2**, **3**, and the lowest energy dissociation channel) at an appropriate level of molecular orbital (MO) theory and (ii) to use an experiment which allows a distinction of **1** and **2**. It will be shown in the following that this combined theoretical/experimental approach provides evidence that both the fluorine and nitrogen protonated isomers of $[\text{N},\text{F}_3,\text{H}]^+$, $\text{F}_2\text{N}-\text{FH}^+$ (**1**) and F_3NH^+ (**2**), are indeed viable, distinct species in the gas phase.

To this end, ab initio MO calculations, using the recently developed GAUSSIAN-1 level of theory,⁴ have been performed for assessing the structure, stability, and the interconversion and dissociation processes of $[\text{N},\text{F}_3,\text{H}]^+$ isomers. In addition, $[\text{N},\text{F}_3,\text{H}]^+$ ions were obtained in the gas phase, by protonation of NF_3 in a chemical ionization (CI) source, with Brønsted acids of different strength (H_3^+ , D_3^+ , and CH_5^+), and their unimolecular metastable (MI) and collision-induced dissociation patterns were investigated by metastable ion kinetic energy (MIKE)⁵ and collisional activation (CA)⁶ mass spectrometry. While these techniques turned out not suitable to distinguish **1** and **2**, it will be demonstrated that the structural assessment of the $[\text{N},\text{F}_3,\text{H}]^+$ connectivities is provided by the determination of the kinetic energy release (KER), associated with the process $[\text{N},\text{F}_3,\text{H}]^+ \rightarrow \text{NF}_2 + \text{HF}$ and the analysis of these data in terms of the ab initio calculated potential energy surface of $[\text{N},\text{F}_3,\text{H}]^+$ ions.

Computational Details

Ab initio quantum-mechanical calculations were performed by using a CONVEX 230 and a CRAY X-MP version of the GAUSSIAN 88 program package.⁷ The standard internal 6-31G*,^{8a}

6-31G**,^{8b} 6-311G**,^{8b} 6-311+G**,^{8c} and 6-311G**(2df)^{8c} basis sets were employed throughout. Geometry optimizations were performed in the full space of coordinates by using analytical gradient based techniques⁹ in the framework of the second-order Møller-Plesset (MP2) perturbation theory,¹⁰ employing the 6-31G** basis set. The MP2 theory was used with full (FU) electron correlation, including inner-shell electrons. The geometries obtained in this way are denoted as MP2(FU)/6-31G**. The vibrational frequencies, at the SCF 6-31G* level of theory, were computed for all of the investigated species, in order to characterize them as true minima, transition structures, or higher-order saddle points on the corresponding potential energy hypersurfaces. Due to known inadequacies in frequencies calculated at this level of theory,¹¹ the obtained values were uniformly scaled by a factor of 0.893, and the zero-point vibration energies (ZPVE's) of the various species were taken into account in this way. Single-point calculations, at the post-SCF level of theory, were performed within the Møller-Plesset framework up to the fourth order (MP4), by including single, double, triple, and quadruple excitations. A post-MP4 correction for residual correlation energy contributions was accounted for by quadratic configuration interaction (QCISD).¹² The GAUSSIAN-1 procedure, as outlined in ref 4 was employed to obtain thermochemical data for the investigated processes. This method is generally accepted as a computational procedure which seems to be able to predict or to reproduce thermochemical data to a target accuracy of $\pm 1-2$ kcal mol⁻¹. The performance of this theory is in the investigation of gas-phase ionic processes has been recently reviewed and its suitability amply demonstrated.¹³

In the framework of the GAUSSIAN-1 approach, which can be considered to be equivalent to a post-MP4 level, the correction for residual electron correlation energy effects, not taken into account at the MP4(SDTQ) level of theory, is introduced by quadratic configuration interaction, which is known to reproduce full configuration interaction (FCI) results quite well, particularly near equilibrium geometries.^{12,13} To avoid very extensive calculations at the QCISD(T)/6-311+G**(2df) level of theory, four correction terms are added to the MP4(SDTQ)/6-311G**//MP2(FU)/6-31G** absolute energies. These correspond to (i) the effects of the diffuse sp basis functions and (ii) the higher polarization functions on nonhydrogen atoms for the corrections of residual correlation effects, and further the so-called higher-level corrections. Three additional calculations at the MP4/6-311+G**, MP4/6-311G**(2df), and QCISD(T)/6-311G** level of theory, respectively,⁴ are required in order to obtain such corrections. If the corresponding absolute energies are denoted E_1 , E_2 , and E_3 , the correction terms to the MP4/6-311G** computed value, designated as E_0 , are $\Delta E(+)=E_1-E_0$, $\Delta E(2df)=E_2-E_0$, and $\Delta E(\text{QCISD(T)})=E_3-E_0$, respectively. The final value of the GAUSSIAN-1 energy of a species is then given by the following equation:

$$E(\text{G1}) = E_0 + \Delta E(+) + \Delta E(2df) + \Delta E(\text{QCISD(T)}) + \Delta E(\text{HLC}) + \Delta E(\text{ZPVE})$$

The fourth correction term, $\Delta E(\text{HLC})$, is introduced in a parametric way,⁴ and the fifth correction term, $\Delta E(\text{ZPVE})$, takes into account the zero-point vibrational energy correction. All single-point calculations have been performed at the MP2(FU)/6-31G** optimized geometries. It should be mentioned that the GAUSSIAN-1 procedure requires geometries obtained at the MP2(FU)/6-31G* level. Thus, the energies obtained at the

(2) Lias, S. G.; Bartmess, J. E.; Liebman, J. F.; Holmes, J. L.; Levin, R. D.; Mallard, W. G. *J. Phys. Chem. Ref. Data* **1988**, *17*, Suppl. 1.

(3) McMahon, T. B.; Kebarle, P. *J. Am. Chem. Soc.* **1985**, *107*, 2612. The value quoted in this reference, 140.7 kcal mol⁻¹, has been reevaluated with respect to the CO standard. See ref. 2.

(4) Pople, J. A.; Head-Gordon, M.; Fox, D. J.; Raghavachari, R.; Curtiss, L. A. *J. Chem. Phys.* **1989**, *90*, 5622.

(5) Cooks, R. G.; Beynon, J. H.; Caprioli, R. M.; Lester, G. R. *Metastable Ions*; Elsevier: Amsterdam, 1973.

(6) Reviews: (a) Levens, K.; Schwarz, H. *Angew. Chem., Int. Ed. Engl.* **1976**, *15*, 609. (b) Cooks, R. G., Ed. *Collision Spectroscopy*; Plenum: New York, 1978. (c) Levens, K.; Schwarz, H. *Mass Spectrom. Rev.* **1985**, *3*, 77. (b) Bordas-Nagy, J.; Jennings, K. R. *Int. J. Mass Spectrom. Ion Processes* **1990**, *100*, 105.

(7) Frisch, M. J.; Head-Gordon, M.; Schlegel, H. B.; Raghavachari, K.; Binkley, J. S.; Gonzalez, C.; Defrees, D. J.; Fox, D. J.; Whiteside, R. A.; Seeger, R.; Melius, C. F.; Baker, J.; Martin, R. L.; Rahn, L. R.; Stewart, J. J. P.; Fluder, E. M.; Topiol, S.; Pople, J. A. *GAUSSIAN 88; Gaussian Inc.: Pittsburgh, PA*, 1988.

(8) (a) Hariharan, P. C.; Pople, J. A. *Chem. Phys. Lett.* **1972**, *66*, 217. (b) Krishnan, R.; Binkley, J. S.; Seeger, R.; Pople, J. A. *Chem. Phys. Lett.* **1980**, *72*, 4244. (c) Frisch, M. J.; Pople, J. A.; Binkley, J. S. *J. Chem. Phys.* **1984**, *80*, 3265.

(9) Schlegel, H. B. *J. Comput. Chem.* **1982**, *3*, 214.

(10) Møller, C.; Plesset, M. S. *Phys. Rev.* **1934**, *46*, 618.

(11) Pople, J. A.; Schlegel, H. B.; Krishnan, R.; Defrees, D. J.; Binkley, J. S.; Frish, M. J.; Whiteside, R. A.; Hout, R. F.; Hehre, W. J. *Int. J. Quantum Chem. Symp.* **1981**, *15*, 269.

(12) Pople, J. A.; Head-Gordon, M.; Raghavachari, R. *J. Chem. Phys.* **1987**, *87*, 5968.

(13) (a) Radom, L. *Org. Mass Spectrom.* **1991**, *266*, 359. (b) Ma, N. L.; Smith, B. J.; Pople, J. A.; Radom, L. *J. Am. Chem. Soc.* **1991**, *113*, 7903.

Table I. Total Energies (Atomic Units) for the NF_3 and HF Molecules, the $[\text{N},\text{F}_3,\text{H}]^+$ Isomers 1–3, and the NF_2^+ Ion

species (NIMAG) ^a	MP2/6-31G**	MP4/6-311G**	MP4/6-311+G**	MP4/6-311G** (2df)	QCISD(T)/6-311G**
NF_3 (0)	-353.236 61	-353.463 94	-353.486 69	-353.648 97	-353.459 56
1 (0)	-353.466 64	-353.709 14	-353.725 24	-353.884 28	-353.701 35
2 (0)	-353.468 52	-353.695 96	-353.709 34	-353.879 99	-353.692 24
3 (1)	-353.387 32	-353.619 56	-353.634 02	-353.803 19	-353.609 53
NF_2^+ (0)	-253.240 27	-253.410 74	-253.418 47	-253.538 31	-253.402 92
HF (0)	-100.196 70	-100.274 14	-100.286 11	-100.319 95	-100.273 87

^aNIMAG = number of imaginary frequencies.

Table II. MP4/6-311G** Absolute Energies (Hartrees) and Corrections (Millihartrees) for the Evaluation of the GAUSSIAN-1 Energies (Hartrees) of the NF_3 and HF Molecules, and $[\text{N},\text{F}_3,\text{H}]^+$ Isomers 1–3, and the NF_2^+ Ion^a

species	MP4/6-311G**	$\Delta E(+)$	$\Delta E(2df)$	$\Delta E(QCI)$	$\Delta E(HLC)$	ZPVE	GAUSSIAN-1	RS
NF_3	-353.463 94	-22.75	-185.03	+4.38	-79.82	11.38	-353.735 78	
1	-353.709 14	-16.1	-175.10	+7.79	-79.82	18.64	-353.953 73	0
2	-353.695 96	-13.38	-184.03	+3.72	-79.82	25.90	-353.943 57	+6.4
3	-353.619 56	-14.46	-183.63	+10.03	-79.82	17.50	-535.869 94	+52.6
NF_2^+	-253.410 74	-7.73	-127.57	+7.82	-55.26	7.97	-253.585 51	
HF	-100.274 14	-11.97	-45.81	+0.27	-24.56	8.86	-100.347 35	

^aThe ZPVE (millihartrees) and the relative stability (RS, kcal mol⁻¹) with respect to isomer 1 are also reported.

MP2(FU)/6-31G** level of theory are likely to be very similar but not (as rightly pointed out by a reviewer) the same as the "true" GAUSSIAN-1 energies.

Experimental Section

The experimental setup has been described in detail elsewhere.¹⁴ Briefly, in a modified VG-HF-2F-AMD tandem mass spectrometer of BEBE configuration (B stands for magnetic and E for electric sector), $[\text{N},\text{F}_3,\text{H}]^+$ ions were formed by protonation of NF_3 (Fluorochem. Cim.) with different reagent gases (CH_4 , H_2), in a chemical ionization (CI) source. Typical operating conditions were as follows: NF_3 /reagent gas \approx 1:8, total ion source pressure (housing), 10^{-4} mbar; repeller voltage, ca. 0 V; electron energy, 100 eV; emission current, 0.5 mA; acceleration voltage, 8 keV.

For MI and CA spectra the $[\text{N},\text{F}_3,\text{H}]^+$ ions were mass-selected by means of B(1)E(1) (resolution $m/\Delta m = 3000$; 10% valley definition). The metastable or collision induced fragmentations occurring in the field-free region preceding the second magnet, B(2), were recorded by scanning B(2).

For the determination of the kinetic energy releases (KER's),⁵ the ions were selected by B(1) and the unimolecular reactions occurring in the field-free region between B(1) and E(1) were measured by scanning E(1) (background pressure $< 10^{-8}$ mbar). The energy width of the parent ion beam was ≤ 2 V.

All spectra were accumulated and on-line processed with either the VG 11/250 or the AMD Intetra data system; 10–40 scans were averaged to improve the signal-to-noise ratio.

Theoretical Results

Details of the protonation of NF_3 have been addressed in the past years by ab initio quantum-mechanical calculations.¹ As pointed out in the Introduction, the question of the existence and the relative stability of the two possible structures of $[\text{N},\text{F}_3,\text{H}]^+$, i.e., the fluorine and nitrogen protonated isomers **1** and **2**, has been examined by Fisher and McMahon.^{1a} At the SCF 6-31G** level of theory, after the inclusion of zero-point energy corrections, the fluorine protonated form $\text{F}_2\text{N}-\text{FH}^+$ (**1**) was found to be 2.2 kcal mol⁻¹ more stable than the nitrogen protonated isomer $\text{F}_3\text{N}-\text{H}^+$ (**2**); this order of stability is essentially determined by zero-point energy contributions.^{1a} The fluorine protonated form **1** was found to correspond to an ion/molecule complex¹⁵ between NF_2^+ and HF; this interpretation is indicated, inter alia, by the long distance (2.217 Å) between the two building blocks of **1**. Since the accuracy of the employed theoretical procedure^{1a} is clearly lower than the estimated energy difference between **1** and **2**, the results

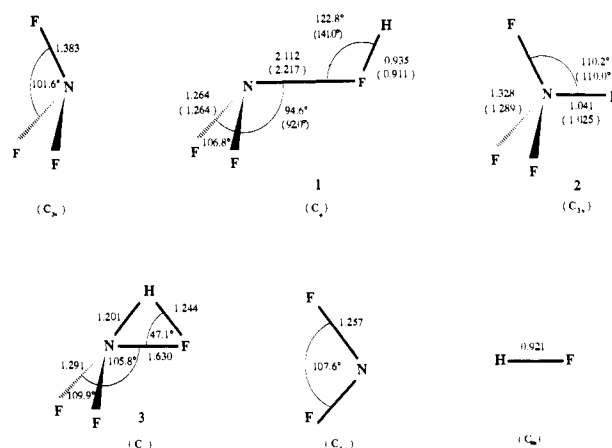


Figure 1. Geometric data (bond length in Å, bond angles in degrees) of NF_3 , $[\text{N},\text{F}_3,\text{H}]^+$, NF_2^+ , and HF. Data given in parentheses are taken from ref 1a and refer to SCF 6-31G** calculations. Our data were calculated at MP2(FU)/6-31G** (see text).

of these calculations cannot furnish a definitive answer to the question of the relative stability of the two isomers of protonated NF_3 . Further, the central question of their possible interconversion barrier has not been previously addressed. Based on these considerations, we decided to theoretically investigate the protonation of NF_3 by employing the more reliable GAUSSIAN-1 theory.^{4,13}

Optimized geometries at the MP2/6-31G** level of theory of the NF_3 molecule, the two $[\text{N},\text{F}_3,\text{H}]^+$ isomers **1** and **2**, and the transition structure **3** connecting **1** and **2** are shown in Figure 1. The structures of NF_2^+ and HF, determined at the same computational level, are also shown for comparison. The relevant data for the evaluation of the GAUSSIAN-1 energies of all the investigated species are given in Tables I and II.

From the structural data given in Figure 1, we note that the inclusion of correlation energy effects in the geometry optimizations does not substantially modify the previously reported¹ SCF 6-31G** structures of **1** and **2** (the latter data are given in parentheses). In particular, fluorine protonation leads, as earlier pointed out,^{1a} to the formation of an ion/molecule complex as indicated by the substantial lengthening of the N–F single bond in the NF_3 molecule.

The data given in Table II serve to discuss the energetics of the protonation of NF_3 , and a schematic view of the two-dimensional potential energy surface of the relative stabilities of the various species is given in Figure 2.

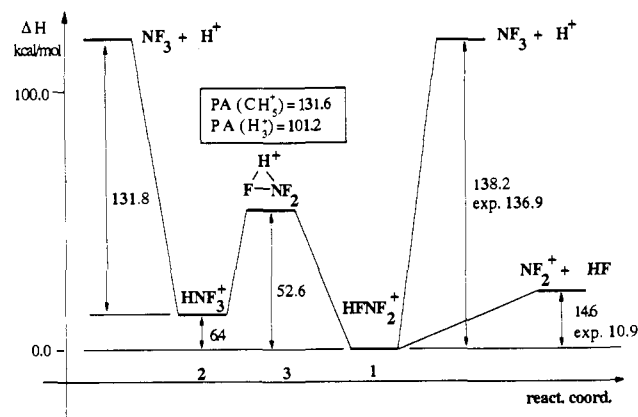
The most stable form of protonated NF_3 is obtained by protonation at the fluorine atom (**1**). The nitrogen-protonated isomer **2** is calculated to be less stable by 6.4 kcal mol⁻¹. This conclusion is qualitatively consistent with the previously reported finding,¹

(14) (a) Srinivas, R.; Sülzle, D.; Weiske, T.; Schwarz, H. *Int. J. Mass Spectrom. Ion Processes* **1991**, *107*, 369. (b) Srinivas, R.; Sülzle, D.; Koch, W.; DePuy, C. H.; Schwarz, H. *J. Am. Chem. Soc.* **1991**, *113*, 5970.

(15) For reviews, see: (a) Morton, T. H. *Tetrahedron* **1982**, *38*, 3195. (b) McAdoo, D. J. *Mass Spectrom. Rev.* **1988**, *7*, 3663. (c) Heinrich, N.; Schwarz, H. In *Ion and Cluster Ion Spectroscopy and Structure*; Maier, J. P., Ed.; Elsevier: Amsterdam, 1989; p 329. (d) Bowen, R. D. *Acc. Chem. Res.* **1991**, *24*, 364.

Table III. CA Mass Spectra^a (He, 80% transmission) of $[\text{N}_2\text{F}_3\text{H}(\text{D})]^+$ Ions Produced from NF_3 and Different Reagent Gases

reagent gas	-H ⁺	-D ⁺	-F ⁺	-HF	-DF	-F ₂	-(HF + F)	-(DF + F)	-NF ₂
CH ₄	<1		2	100		<1	6		1
H ₂	1		2	100		<1	6		1
D ₂	1	1	3		100	<1		6	1

^a Metastable ion contribution less than 1%.**Figure 2.** Schematic view of the potential energy surface of NF_3/H^+ , $[\text{N}_2\text{F}_3\text{H}]^+$, and NF_2^+/HF as calculated by GAUSSIAN-1 (see text and Table II).

but the energy difference is found to be larger at our higher level of theory (6.4 versus 2.2 kcal mol⁻¹).

The data in Table II also reveal the existence of a high-energy barrier for the interconversion 1 → 2 via transition structure 3; at the highest level of theory we obtain a value of 52.6 kcal mol⁻¹ with respect to the global minimum 1. The geometry of the corresponding transition structure 3 is given in Figure 1. A C₁ symmetric structure results, whose imaginary frequency, -2318.9 cm⁻¹, is typical for a 1,2-hydrogen migration process.

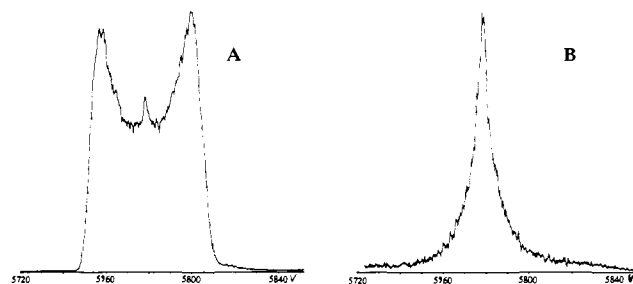
From the energies of NF_3 , 1 and 2, respectively, the 298 K proton affinity of both the fluorine and nitrogen sites of NF_3 can be obtained, after inclusion of thermal energy contributions. As indicated in Figure 2, the nitrogen site has a proton affinity of 131.8 and the fluorine site of NF_3 of 138.2 kcal mol⁻¹, respectively. The agreement between the computed fluorine site PA of NF_3 , giving rise to the formation of the most stable isomer $\text{F}_2\text{N}-\text{FH}^+$ (1), and the experimental determined PA of NF_3 , 136.9 ± 1 kcal mol⁻¹,³ is excellent and leads to the conclusion that the fluorine protonated form of NF_3 is indeed generated under high-pressure mass spectrometric conditions.^{1a,3}

As a final remark in this section, the calculated dissociation enthalpy of ion 1 into NF_2^+ and HF, as obtained from the data of Table II, corresponds to 14.6 kcal mol⁻¹; this number favorably compares with the experimental one (10.9 ± 2 kcal mol⁻¹),² if one takes into account the difficulties in accurately determining the heat of formation of NF_2^+ . For the process $\text{F}_2\text{N}-\text{FH}^+ \rightarrow \text{NF}_2^+ + \text{HF}$ we did not find a reverse activation barrier, and the reaction corresponds to the energetically by far most favored one among all conceivable product combinations.

Mass Spectrometric Results

For the protonation of NF_3 the Brønsted acids H_3^+ , D_3^+ , and CH_5^+ were employed to generate $[\text{N}_2\text{F}_3\text{H}(\text{D})]^+$ ions in the gas phase. It is well known that the strength of the acids affects the exothermicity of the reaction and hence determines the excess energy imparted to the $[\text{N}_2\text{F}_3\text{H}]^+$ ions. In particular, the protonations by H_3^+ and CH_5^+ of NF_3 are predicted to be exothermic by 36 and 5 kcal mol⁻¹, respectively,^{2,3} if the thermochemically favored $[\text{N}_2\text{F}_3\text{H}^+]$ isomer 1 is generated.¹⁶

(16) Obviously, the excess energy imparted to $[\text{N}_2\text{F}_3\text{H}]^+$ corresponds to an upper limit due to (i) the non-equilibrium conditions in a "low-pressure" CI source and (ii) the kinetic energy carried off by the neutral B in the reaction $\text{NF}_3 + \text{BH}^+ \rightarrow [\text{N}_2\text{F}_3\text{H}]^+ + \text{B}$. In reality, $[\text{N}_2\text{F}_3\text{H}]^+$ will be formed with an (unknown) distribution of energy.

**Figure 3.** Kinetic energy releases (KER's) for the reaction $[\text{N}_2\text{F}_3\text{H}]^+ \rightarrow \text{NF}_2^+ + \text{HF}$: (A) protonation of NF_3 with H_3^+ ; (b) protonation of NF_3 with CH_5^+ .

Initially, we have employed MIKE and CA mass spectrometry to probe the populations of $[\text{N}_2\text{F}_3\text{H}]^+$ ions using different protonation conditions. However, the only observed metastable ion MI decomposition of the $[\text{N}_2\text{F}_3\text{H}]^+$ ions, irrespective of their formation process, corresponds to the loss of HF.¹⁷ This observation is in keeping with the theoretical result in that (i) elimination of HF is the energetically most favored reaction channel and (ii) all other conceivable dissociation processes of $[\text{N}_2\text{F}_3\text{H}]^+$ have energy requirements exceeding the internal energy imparted to $[\text{N}_2\text{F}_3\text{H}]^+$ in the course of protonation of NF_3 by BH^+ (B = H_2 , CH_4). The CA mass spectra of $[\text{N}_2\text{F}_3\text{H}]^+$ are also practically identical (Table III), irrespective of the Brønsted acid used. The spectra are dominated by loss of HF.

However, the kinetic energy release measurements reveal a dramatic difference with respect to the nature of the protonating species, e.g., H_3^+ or CH_5^+ . The corresponding MIKE spectra are given in Figure 3, A and B. The ions $[\text{N}_2\text{F}_3\text{H}]^+$ generated in the reaction of H_3^+ with NF_3 show a composite, dished-top peak (Figure 3A) with a kinetic energy release, $T_{<0.5>}$, of 740 meV (768 meV when D_3^+ is used) and a narrow central component. On protonation with CH_5^+ , it is only this central component which is observed; the kinetic energy release corresponds to $T_{<0.5>} = 21$ meV (Figure 3B). Such a difference is particularly significant, in that large kinetic energy releases and non-Gaussian peak shapes are generally indicative of high reverse activation energies, typical of those fragmentation processes that require prior rearrangement of the decomposing ions, while direct bond cleavages (continuously endothermic processes) have little or no reverse activation energies and often give rise to small KER data and Gaussian-type signals.^{5,18}

Discussion

Both the MO calculations and the KER data point to the existence of two distinct, non-interconvertible $[\text{N}_2\text{F}_3\text{H}]^+$ isomers, and a coherent description of the experimental findings is easily provided in terms of the PA's of H_2 , CH_4 , and NF_3 and the potential energy surface depicted in Figure 2.

For the sake of clarity we will discuss the protonation of NF_3 with CH_5^+ and H_3^+ separately. Upon protonation with CH_5^+ both isomers $\text{F}_2\text{N}-\text{FH}^+$ (1) and $\text{F}_3\text{N}-\text{H}^+$ (2) will be formed, and under multiple-collision, i.e., in a high-pressure experiment,³ it is the

(17) The MI spectra of $[\text{N}_2\text{F}_3\text{H}]^+$ ions in the second field-free region preceding E(1) show an additional signal due to "F-atom" loss. However, this signal is actually caused by an artifact due to the decomposition of isobaric ¹⁵NF₃⁺. This is demonstrated by either recording the MI spectra of "pure" [¹⁴N₂F₃H]⁺ using B(1)E(1) for the mass-selection or recording the MI spectra of [¹⁴N₂F₃D]⁺ using B(1) for the mass-selection.

(18) (a) Holmes, J. L.; Terlouw, J. K. *Org. Mass Spectrom.* **1980**, *15*, 393. (b) Holmes, J. L. *Org. Mass Spectrom.* **1985**, *20*, 1669. (c) Bowen, R. D.; Williams, D. H.; Schwarz, H. *Angew. Chem., Int. Ed. Engl.* **1979**, *18*, 451.

thermochemically more stable isomer **1** which eventually emerges as the only "detectable" isomer. In our experiment, **1** and **2** are also simultaneously generated with a range of little excess energy. Due to the high barriers for isomerization or (direct)¹⁹ dissociation, the isomer F_3N-H^+ (**2**) is trapped in a deep potential well; hence, it will not give rise to a metastable ion decomposition. In contrast, a portion of the fluorine-protonated isomer F_2N-FH^+ has enough internal energy to undergo time-delayed dissociation to NF_2^+ and HF. As indicated in Figure 2, the energy necessary to bring about this process is $<14.6 \text{ kcal mol}^{-1}$. If one takes into account the contribution of the thermal energy of the system, this energy demand is provided for part of the F_2N-FH^+ ion population in the protonation NF_3 with CH_3^+ . Most importantly, as there is no reverse activation energy and the excess energy is small, a metastable ion peak with a small kinetic energy release results, as shown in Figure 3B.

A fundamentally different situation prevails if H_3^+ is used in the protonation of NF_3 . Again, first principle considerations suggest that the proton will be transferred to either site of NF_3 ; i.e., both F_2N-FH^+ (**1**) and F_3N-H^+ (**2**) will be formed. However, in contrast to the reaction employing CH_3^+ , the internal energy of the so-formed ions **1** and **2** will be much higher. This has two implications. (i) Most of the fluorine-protected ions will already dissociate in the ion source, and only a small, low-energy fraction will have a lifetime such that dissociation in the second or third field-free region will occur. Consequently, the fraction of this process to the composite peak (narrow component of Figure 3A) is quite small. (ii) F_3N-H^+ is now formed with internal energy high enough that a portion can overcome the barrier imposed by the transition structure **3**¹⁹ to eventually dissociate (from vibra-

tionally/rotationally excited **1**) to NF_2^+ and HF. In view of previous findings,^{5,13,18} it is not unreasonable to argue that the tight transition structure **3** and the large energy difference between **3** and the products NF_2^+/HF (ca. 39 kcal mol^{-1}) result in the dished-top peak as shown in Figure 3A. It goes without saying that, based on the potential energy surface depicted in Figure 2, a more refined picture will emerge by performing appropriate ion/trajectory calculations.

In conclusion, the combined theoretical/experimental approach employed in this study demonstrates that both the fluorine and the nitrogen protonated form of NF_3 are distinct species in the gas phase. Both ions are separated by a significant barrier ($52.6 \text{ kcal mol}^{-1}$) which prevents facile interconversion. The global minimum corresponds to the fluorine protonated isomer F_2N-FH^+ (**1**), which can be viewed as an ion/dipole complex. The nitrogen-protonated form F_3N-H^+ (**2**) is $6.4 \text{ kcal mol}^{-1}$ less stable. While the former isomer has a low-energy dissociation channel to produce NF_2^+ and HF (theory, $14.6 \text{ kcal mol}^{-1}$; experimental data, $10.9 \text{ kcal mol}^{-1}$), the isomer F_3NH^+ (**2**) is trapped in a deep potential well, which prevents both rapid isomerization and dissociation. It is this particular aspect of the potential energy surface which explains the different kinetic energy releases (KER's) data obtained from the dissociation of **1** and **2**: HF loss from F_2N-FH^+ (**1**) gives rise to a small KER (21 meV, Figure 3B), while the same reaction of F_3NH^+ (**2**) is associated with a dished-top peak (Figure 3A) and a large KER (740 meV).

Acknowledgment. The generous financial support of our work by the Fonds der Chemischen Industrie, the Deutsche Forschungsgemeinschaft, and the Gesellschaft von Freunden der Technischen Universität Berlin is gratefully appreciated. F.G. is indebted to the Consiglio Nazionale delle Ricerche (CNR) of Italy for a visiting fellowship.

(19) It was not possible to locate a transition structure for the direct elimination of HF from F_3N-H^+ (**2**).

Conformational Analysis. 15. 1,2-Dibromotetrafluoroethane and 1,2-Diiodotetrafluoroethane. Electron Diffraction Investigations of the Molecular Structures, Compositions, and Anti-Gauche Energy and Entropy Differences

Hanne Thomassen, Svein Samdal,[†] and Kenneth Hedberg*

Contribution from the Department of Chemistry, Oregon State University, Corvallis, Oregon 97331. Received September 17, 1991

Abstract: The molecular structures and conformational compositions of 1,2-dibromotetrafluoroethane (DBTF) and 1,2-diiodotetrafluoroethane (DITF) have been investigated in the gas phase by electron diffraction each at three nozzle-tip temperatures: DBTF, 273, 388, and 673 K; DITF, 293, 393, and 473 K. Both molecules exist as a mixture of anti and gauche rotamers with the former the more stable. Distances ($r_e/\text{\AA}$) and angles (\angle_e/deg) for the lowest temperatures, with estimated 2σ uncertainties, are as follows: (DBTF) $r(C-F) = 1.340$ (3), $r(C-C) = 1.559$ (13), $r(C-Br) = 1.930$ (5), $\angle CCF = 109.9$ (4), $\angle FCF = 108.4$ (8), $\angle CCB_r = 110.5$ (5), and $\angle BrCCBr_G = 67$ (3); (DITF) $r(C-F) = 1.334$ (3), $r(C-C) = 1.542$ (13), $r(C-I) = 2.146$ (7), $\angle CCF = 109.1$ (6), $\angle FCF = 108.2$ (7), $\angle CCI = 111.7$ (6), and $\angle ICCI_G = 70$ (3). The rotameric compositions of DBTF at 273, 388, and 673 K were found to be 30 (8), 39 (14), and 53 (18) % gauche, from which the energy and entropy differences are calculated to be $E_G^\circ - E_A^\circ = 3.6$ (11) kJ/mol and $S_G^\circ - S_A^\circ + R \ln 2 = 6.0$ (34) J/(mol·K). For DITF at 298, 393, and 473 K, the compositions are 19 (6), 24 (11), and 35 (13) % gauche from which the energy and entropy differences are $E_G^\circ - E_A^\circ = 5.1$ (15) kJ/mol and $S_G^\circ - S_A^\circ + R \ln 2 = 5.0$ (44) J/(mol·K). The structures and thermodynamic properties are discussed.

Introduction

Ethanes substituted in the 1,2 positions exist as mixtures of anti and gauche conformers as a result of rotation around the C-C bond. In the dihalogenated ethanes 1,2-dichloro-,¹ 1,2-dibromo-,²

and 1,2-diiodoethane,³ the predominance of the anti over gauche can be explained by steric effects. In 1,2-difluoroethane the gauche

(1) Kveseth, K. *Acta Chem. Scand., Ser. A* 1975, 29, 307. Kveseth, K. *Ibid.* 1974, 28, 482.

(2) Kveseth, K. *Acta Chem. Scand., Ser. A* 1978, 32, 63.

(3) Samdal, S.; Hedberg, K. Unpublished results.

[†] Present address: Oslo College of Engineering, Cort Adelers gt. 30, N-0254, Oslo 2, Norway.